TRPC1 binds to caveolin-3 and is regulated by Src kinase – role in Duchenne muscular dystrophy

Othon L. Gervásio[1], Nicholas P. Whitehead[1], Ella W. Yeung[2], William D. Phillips[1] and David G. Allen[1,*]

[1]School of Medical Sciences, Discipline of Physiology (F13), Bosch Institute, The University of Sydney, NSW 2006, Australia
[2]Department of Rehabilitation Sciences, Hong Kong Polytechnic University, Hung Hom, Kowloon, Hong Kong
*Author for correspondence (e-mail: davida@physiol.usyd.edu.au)

Accepted 22 April 2008
Journal of Cell Science 121, 2246-2255 Published by The Company of Biologists 2008
doi:10.1242/jcs.032003

Summary

Transient receptor potential canonical 1 (TRPC1), a widely expressed calcium (Ca^{2+})-permeable channel, is potentially involved in the pathogenesis of Duchenne muscular dystrophy (DMD). Ca^{2+} influx through stretch-activated channels, possibly formed by TRPC1, induces muscle-cell damage in the *mdx* mouse, an animal model of DMD. In this study, we showed that TRPC1, caveolin-3 and Src-kinase protein levels are increased in *mdx* muscle compared with wild type. TRPC1 and caveolin-3 colocalised and co-immunoprecipitated. Direct binding of TRPC1-CFP to caveolin-3–YFP was confirmed in C2 myoblasts by fluorescence energy resonance transfer (FRET). Caveolin-3–YFP targeted TRPC1-CFP to the plasma membrane. Hydrogen peroxide, a reactive oxygen species (ROS), increased Src activity and enhanced Ca^{2+} influx, but only in C2 myoblasts co-expressing TRPC1 and caveolin-3. In *mdx* muscle, Tiron, a ROS scavenger, and PP2, a Src inhibitor, reduced stretch-induced Ca^{2+} entry and increased force recovery. Because ROS production is increased in *mdx*/DMD, these results suggest that a ROS-Src-TRPC1/caveolin-3 pathway contributes to the pathogenesis of *mdx*/DMD.

Supplementary material available online at
http://jcs.biologists.org/cgi/content/full/121/13/2246/DC1

Key words: Duchenne muscular dystrophy, Src, TRPC1, Caveolin-3, *mdx*

Introduction

Transient receptor potential canonical 1 (TRPC1) was the first of seven mammalian TRPC calcium (Ca^{2+}) channels to be identified, and is widely expressed in tissues (Liu et al., 2000; Rao et al., 2006; Sours et al., 2006), including in cardiac (Williams and Allen, 2007a; Ju et al., 2007) and skeletal (Vandebrouck et al., 2002; Venkatachalam and Montell, 2007) muscles. TRPC1 can be activated by protein kinase C (Ahmmed et al., 2004), STIM1 (Huang et al., 2006), membrane stretch (Maroto et al., 2005) and depletion of Ca^{2+} stores (Sinkins et al., 1998). Even though many studies point to TRPC1 as being a store- and stretch-activated channel (SOC and SAC, respectively) (Ducret et al., 2006), this topic remains controversial, with tissue-specific investigations of TRPC1 function often providing negative results (Brereton et al., 2000; Dietrich et al., 2007; Gottlieb et al., 2008).

Regulatory proteins, such as caveolins, could also be involved in the regulation of TRPC1. In cells that express caveolin-1 (salivary gland and kidney), caveolin-1 binds to TRPC1, promotes its assembly into channels and regulates its activity (Brazer et al., 2003). Caveolins are the scaffolding proteins of caveolae – 20-50 nm invaginations of the cell surface enriched with specific lipids (glycosphingolipids, sphingomyelin and cholesterol) and lipid-modified signalling molecules (Engelman et al., 1998). Caveolins play an important role in signalling pathways because they bind to and regulate the activity of many proteins (for a review, see Williams and Lisanti, 2004). Caveolin-3, the muscle-specific caveolin isoform, seems to play an important role in muscle physiology. Mutations that reduce expression of the caveolin-3 gene cause limb-girdle muscular dystrophy (Minetti et al., 1998). Transgenic overexpression of caveolin-3 induces a phenotype similar to Duchenne muscular dystrophy (DMD) (Galbiati et al., 2000). DMD is a degenerative muscle disease caused by the absence of dystrophin, a membrane-anchoring protein that provides a mechanical link from the intracellular cytoskeleton to the extracellular matrix (Hoffman et al., 1987). Vaghy and colleagues also found higher levels of caveolin-3 in muscles of *mdx* mice, an animal model of DMD (Vaghy et al., 1998).

Both caveolin-3 and TRPC1 bind to Src kinase (Li et al., 1996; Kawasaki et al., 2006). The Src-kinase family is expressed in many cell types, including muscle (Abram and Courtneidge, 2000). Src kinase regulates many cellular events such as cell proliferation, cytoskeletal organisation, differentiation, survival, adhesion and migration (Thomas and Brugge, 1997). Members of the Src-kinase family can phosphorylate TRPC3 (Kawasaki et al., 2006) and TRPC6 (Hisatsune et al., 2004); however, regulation of TRPC1 activity by Src has not been investigated. Src kinase has been shown to be activated by reactive oxygen species (ROS), such as hydrogen peroxide (H_2O_2) (Chen et al., 2005), and TRPC3 activity is increased by ROS (Poteser et al., 2006). Thus, it is possible that ROS-induced Src activation, leads to phosphorylation and activation of transient receptor potential canonical (TRPC) channels.

TRPC1 has been associated with many pathologies in which Ca^{2+} homeostasis is disturbed (Sweeney et al., 2002; Kumar et al., 2006; Pani et al., 2006), including DMD (Vandebrouck et al., 2002; Vandebrouck et al., 2007; Williams and Allen, 2007a). Reports of increased intracellular Ca^{2+} concentration ($[Ca^{2+}]_i$) in dystrophin-deficient cells have led to the hypothesis that the muscle damage and degeneration in DMD are a consequence of activation of Ca^{2+}-dependent proteases, particularly calpains (Spencer et al., 1995; Mariol and Ségalat, 2001). TRPC1 has been proposed as one of

the possible causes of increased $[Ca^{2+}]_i$ in *mdx* muscle. Expression of TRPC1 is increased in *mdx* cardiac muscle (Williams and Allen, 2007a), and repression of TRPC1 by siRNA decreases both SOC and SAC occurrence and activity in *mdx* skeletal muscle cells (Vandebrouck et al., 2002). We have shown that SACs cause increased Ca^{2+} influx into *mdx* fibres when the fibres are stretched during active contractions (Yeung et al., 2005), and it is therefore plausible that TRPC1 channels mediate this Ca^{2+} entry. We have also recently shown that ROS contribute to stretch-induced muscle damage in *mdx* mice (Whitehead et al., 2008). Therefore, it is possible that ROS increase SAC- and/or TRPC1-mediated Ca^{2+} influx in *mdx* muscle, an idea supported by recent findings in *mdx* cardiac cells (Jung et al., 2008).

On the basis of the high degree of homology between caveolin-1 and caveolin-3 (Tang et al., 1996) and previous reports that caveolin-1 binds to TPRC1 (Lockwich et al., 2000; Brazer et al., 2003), we investigated the interaction of caveolin-3 and TRPC1 and how this regulates TRPC1 activity. The role of Src kinase, another TRPC1 binding partner, and its possible activation by ROS was also investigated. Here, we provide evidence that a Ca^{2+}-influx pathway involving ROS, Src, TRPC1 and caveolin-3 might contribute to the elevated $[Ca^{2+}]_i$ that is characteristic of *mdx*/DMD skeletal muscle.

Results

TRPC1, caveolin-3 and Src kinase levels are increased in *mdx* muscle

Western blot analysis showed that TRPC1, caveolin-3 and Src kinase levels were all increased in total lysates of tibialis anterior (TA) muscle of *mdx* mice, compared with wild type (WT) ($P<0.001$ for caveolin-3, and $P<0.05$ for TRPC1 and Src; Fig. 1). To investigate whether TRPC1 and caveolin-3 levels were increased at the sarcolemma, muscle cryosections from *mdx* and WT mice were double labelled for caveolin-3 and TRPC1. Quantitation of immunofluorescence intensity in the sarcolemma region revealed an increase of both proteins in *mdx* muscle (caveolin-3, $P<0.001$; TRPC1, $P<0.05$; Fig. 2) relative to WT. This is consistent with previous reports showing similar increases in protein levels for TRPC1 in *mdx* heart (Williams and Allen, 2007a) and caveolin-3 in *mdx* skeletal muscle (Vaghy et al., 1998). Caveolin-3 and TRPC1 showed a similar sarcolemma labelling pattern, consistent with the hypothesis that these proteins can interact. Double labelling of cryosections of *mdx* and WT muscle were then used to compare the degree of colocalisation (Fig. 3A-F). Binary images of each labelled protein were generated and overlaid (see Materials and Methods; Fig. 3F,G). White pixels in the overlaid image represent colocalisation, independent of fluorescence intensity (Gervásio and Phillips, 2005) (Fig. 3G). Quantification showed that over 50% of caveolin-3 and TRPC1 colocalised in the sarcolemma, in both WT and *mdx* groups (Fig. 3H).

TRPC1 and caveolin-3 interact directly in skeletal muscle

Image analysis revealed a close spatial relationship between caveolin-3 and TRPC1 (Fig. 3A-H). To further investigate the interaction between caveolin-3 and TRPC1, we used co-immunoprecipitation. TA muscles were homogenised in immunoprecipitation (IP) buffer and the lysate was incubated with anti-TRPC1. Immunocomplexes were resolved by SDS-PAGE and the membranes were then probed for caveolin-3. Immunoblots showed that TRPC1 and caveolin-3 co-immunoprecipitated (Fig. 3I,J). Experiments using muscles from WT and *mdx* mice showed that caveolin-3 and TRPC1 co-immunoprecipitated in each case (Fig. 3J). In order to confirm that the detected band represented caveolin-3 and not a background signal from the immunoprecipitating antibody (Kelly et al., 2007), negative controls with no anti-TRPC1 antibody or no lysate were used (Fig. 3I). The reverse IP (IP with anti-caveolin-3 and immunoblot probed with

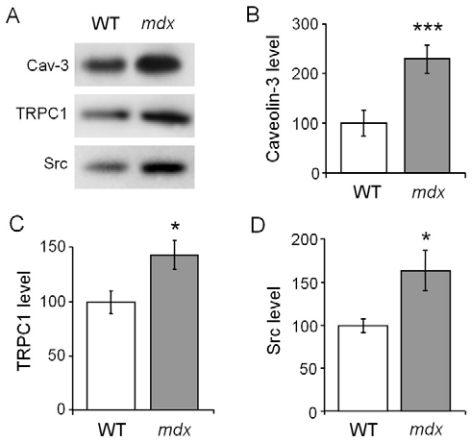

Fig. 1. Levels of caveolin-3, TRPC1 and Src are increased in *mdx* muscle. (A) Sample immunoblots of TA muscle from *mdx* and WT mice. Membranes were probed for caveolin-3, TRPC1 and Src. (B-D) Total lysate (20 µg; Bradford assay) was resolved by SDS-PAGE. Bands were quantified and normalised to GAPDH (see Materials and Methods). Quantitation revealed that levels of caveolin-3, TRPC1 and Src were all increased in the *mdx* group. $n=8$ mice per group. *$P<0.05$; ***$P<0.001$.

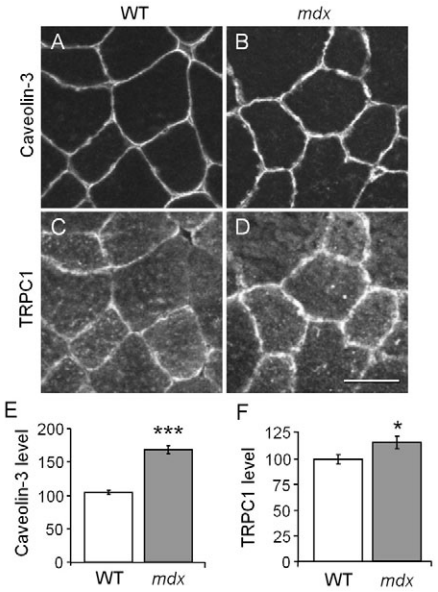

Fig. 2. Sarcolemma levels of TRPC1 and caveolin-3 are increased in *mdx* muscle. (A-D) Sample micrographs of muscle cryosections from WT and *mdx* mice double stained by immunofluorescence for TRPC1 and caveolin-3. Scale bar: 50 µm. (E,F) Quantitation of the fluorescence in the sarcolemma region revealed increased intensity of staining for both TRPC1 and caveolin-3 in the *mdx* group. $n=4$ mice per group, 15 membrane segments per mouse. *$P<0.05$; ***$P<0.001$.

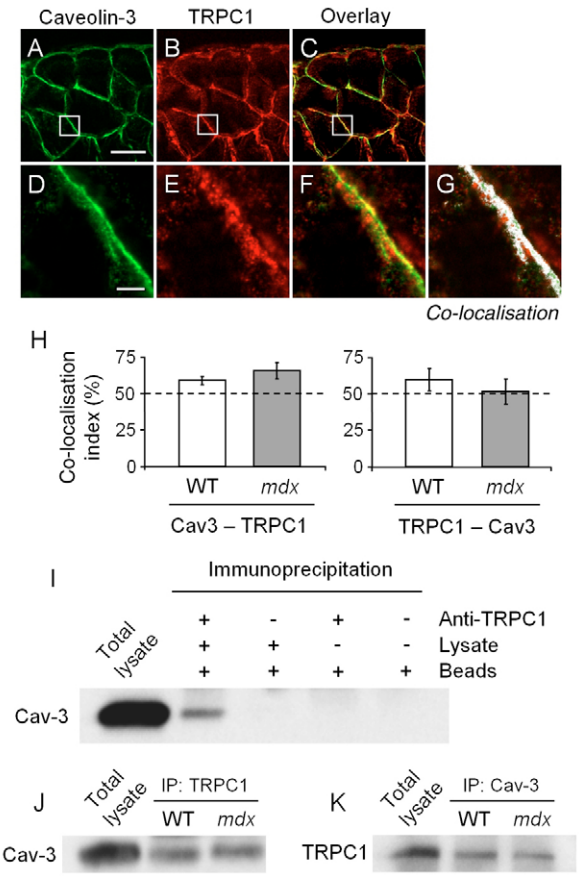

Fig. 3. TRPC1 colocalises and co-immunoprecipitates with caveolin-3. (A-H) Skeletal-muscle cryosections (TA) from *mdx* and WT mice were double labelled for TRPC1 (red) and caveolin-3 (green) (A-F). Images were then overlaid (C,F) and the colocalisation was quantified. (D-F) Higher-magnification images of the insets shown in A-C. Scale bars: A, 50 μm; D, 5 μm. (G) White pixels represent true colocalisation and were compared to the binary images generated from each labelling (data not shown; see Materials and Methods). Staining of caveolin and TRPC1 showed substantial but not complete overlap. (H) More than 50% of TRPC1-stained pixels colocalised with caveolin-3 staining in the sarcolemma and subsarcolemmal compartment, and vice-versa, in both *mdx* and WT groups. In addition, a subset of TRPC1 staining appeared to be associated with punctate subsarcolemmal structures that stained weakly with anti-caveolin3. Mean ± s.e.m. of ten membrane segments per mouse is represented, from three mice per group. (I-K) Co-immunoprecipitation of TRPC1 and caveolin-3. Total lysate from *mdx* and WT skeletal muscle was pre-cleared with agarose beads and incubated with anti-TRPC1. Immunocomplex was resolved by a SDS-PAGE and membranes were probed for caveolin-3. (I,J) Caveolin-3 co-immunoprecipitates with TRPC1 in both *mdx* and WT skeletal muscles. (K) A reverse IP also confirmed that caveolin-3 and TRPC1 co-immunoprecipitate. (I) As negative controls, samples were processed without the primary antibody (anti-TRPC1) or without the lysate. Lysate of a WT mouse was used for the IP.

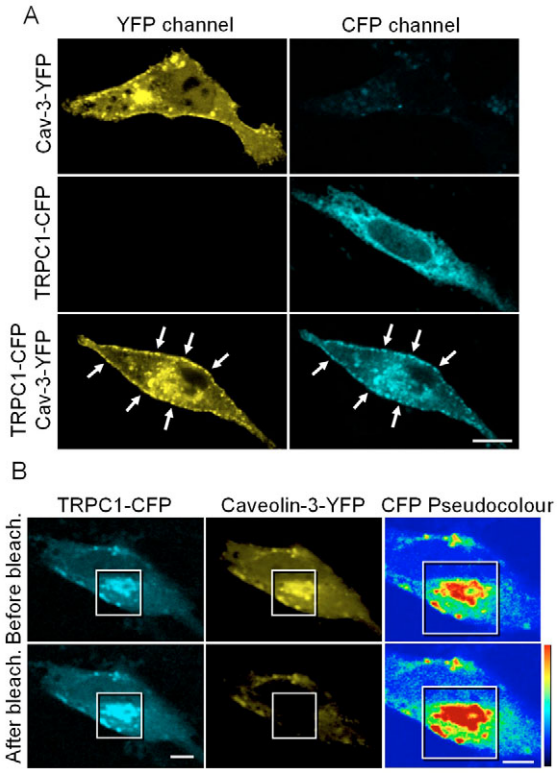

Fig. 4. Caveolin-3 binds to TRPC1 and regulates its plasma membrane localisation. (A) C2 cells were transfected with either TRPC1-CFP, caveolin-3–YFP or the combination of both plasmids. Caveolin-3–YFP targeted to the plasma membrane when transfected either alone or with TRPC1. However, when TRPC1-CFP was transfected alone, it did not target to the plasma membrane and rather showed a diffuse cytoplasmic distribution. TRPC1 was only able to target to the membrane when co-transfected with caveolin-3–YFP (arrows). (B) TRPC1 binds to caveolin-3 (FRET – photobleaching of acceptor). TRPC1-CFP and caveolin-3–YFP were co-transfected into C2 myoblasts. A selected region of caveolin-3–YFP was chosen and photobleached using the 514 nm laser line (100% power). CFP fluorescence increased ~21% (FRET efficiency) upon YFP photobleaching. Scale bars: A, 10 μm; B, 5 μm.

anti-TRPC1) also showed that caveolin-3 and TRPC1 co-immunoprecipitated (Fig. 3K).

To test whether TRPC1 and caveolin-3 interact directly, we transfected TRPC1-CFP (cyan fluorescent protein) and caveolin-3–YFP (yellow fluorescent protein) into C2 myoblasts. Caveolin-3–YFP was expressed both in the cytoplasm and at the cell surface (Fig. 4A). Cells transfected with TRPC1-CFP only showed diffuse cytoplasmic expression of the protein, even though these cells express low levels of caveolin-1 (Galbiati et al., 1999). The levels of endogenous caveolin-1 might be insufficient to target the overexpressed TRPC1 to the plasma membrane in this system. When co-transfected with caveolin-3–YFP, TRPC1-CFP re-distributed to the plasma membrane. In myoblasts transfected with both proteins, a high degree of colocalisation was found between caveolin-3–YFP and TRPC1-CFP, both intracellularly and at the plasma membrane (Fig. 4A).

It has been shown that immunoprecipitation of caveolae-rich microdomains (using anti-caveolin-1 antibody) does not necessarily only reveal caveolin binding partners but can also reveal other proteins present in this lipid raft environment (Zheng and Bollinger Bollag, 2003). To test whether the interaction was likely to be a direct one, we performed fluorescence resonance energy transfer (FRET) using two independent approaches: photobleaching of acceptor, and fluorescence lifetime imaging microscopy (FLIM; see Materials and Methods). C2 myoblasts were transfected with either TPRC1-CFP or caveolin-3–YFP, or both. In cells transfected with both expression plasmids, photobleaching of the acceptor fluorophor (caveolin-3–YFP) increased the fluorescence intensity of the donor (TRPC1-CFP). Because the Förster distance of this FRET pair is 4.9 nm (and defines the distance of a FRET pair in which transfer is 50% efficient) (Patterson et al., 2000), the FRET

efficiency calculated here (21%±0.01, n=10 cells) suggests that the two tag proteins were 6.1 nm from each other (Bastiaens et al., 1996; Gervásio et al., 2007) (Fig. 4B). Photobleaching using the 514 nm laser line of samples transfected either with TRPC1-CFP or caveolin-3–YFP alone resulted in no increase of the fluorescence in the CFP channel (supplementary material Fig. S1). In FLIM, the lifetime of the donor (CFP) is reduced when in close proximity to its FRET partner (YFP, acceptor) (Cox et al., 2007). The lifetime of CFP in C2 cells transfected with TRPC1-CFP alone was 2.7±0.03 nanoseconds (ns) (Fig. 5A-C). When cells were co-transfected with both TRPC1-CFP and caveolin-3–YFP plasmids, the lifetime of the CFP was reduced to 2.17±0.03 ns (P<0.001). This equates to a FRET efficiency of 19.6%. Thus, both photobleaching of acceptor and FLIM support the idea that TRPC1 and caveolin-3 bind directly.

TRPC1 activity depends on caveolin-3 expression and Src phosphorylation

Previous reports have shown that: (1) caveolin-1 regulates TRPC1 channel assembly and activity (Brazer et al., 2003), (2) Src binds to caveolin-3 and to members of the TRPC family (Song et al., 1996; Kawasaki et al., 2006) and (3) Src activates TRPC3 (Vazquez et al., 2004). These findings led us to investigate the effect of caveolin-3 and Src kinase on TRPC1 activity. Given that Src kinase is activated by H_2O_2 in various cell types (Sato et al., 2001; Chen et al., 2001; Suzaki et al., 2002), we first tested whether H_2O_2 would activate endogenous Src in cultured C2 cells, and whether PP2 (a Src-kinase inhibitor) would prevent such activation. C2 cells were incubated with 10 µM H_2O_2 for 15 minutes followed by western blot analysis. The membranes were probed with antibodies against Src and pY418-Src, the active form of Src. H_2O_2 induced close to a twofold increase of the active form of Src (P<0.01; Fig. 6). This increase was completely blocked when cells were pre-incubated with 10 µm PP2 (P<0.05).

We then activated Src with H_2O_2 in cells transfected with TRPC1-CFP and caveolin-3–YFP. FLIM analysis showed that H_2O_2 (and presumably Src activation) resulted in an increase of the CFP lifetime when cells were co-transfected with TRPC1-CFP and caveolin-3–YFP (from 2.17 to 2.33±0.03 ns; P<0.001; Fig. 5D). This increase was prevented when cells were incubated with PP2, confirming the involvement of Src. The change in the CFP lifetime could represent a molecular reorganisation of TRPC1, or a change in its interaction with caveolin-3 (see Discussion).

The activity of TRPC1 upon Src activation was assessed by Ca^{2+} imaging. Fura Red was chosen because of its emission spectrum (far red), which does not interfere with the fluorescence of CFP and YFP. In addition, Fura Red being a ratiometric Ca^{2+} probe, estimation of Ca^{2+} concentration is not affected by probe loading, bleaching or illumination intensity. Myoblasts transfected with either TRPC1-CFP, caveolin-3–YFP or a combination of both plasmids were loaded with Fura Red and imaged with confocal microscopy. The resulting concentration of $[Ca^{2+}]_i$ is shown as a ratio of the fluorescence emission (Fig. 7A, lower graph) upon excitation using 458 nm and 488 nm laser lines (Fig. 7A, upper graph). When H_2O_2 was applied to the cultures, an increase in the $[Ca^{2+}]_i$ was detected, but only in cells transfected with TRPC1-CFP and caveolin-3–YFP (P<0.001; Fig. 7B,C). Cells transfected with caveolin-3–YFP (data not shown) or TRPC1-CFP (Fig. 7C) alone did not show a statistically significant $[Ca^{2+}]_i$ increase with H_2O_2. In order to assess the participation of Src kinase on TRPC1 activity, cells co-transfected with both TRPC1-CFP and caveolin-3–YFP plasmids were incubated with PP2 1 hour prior to H_2O_2. PP2 abolished the rise in $[Ca^{2+}]_i$ in such cells (P<0.001; Fig. 7C). These results suggest that activation of Src by ROS increases TRPC1–caveolin-3-dependent Ca^{2+} influx.

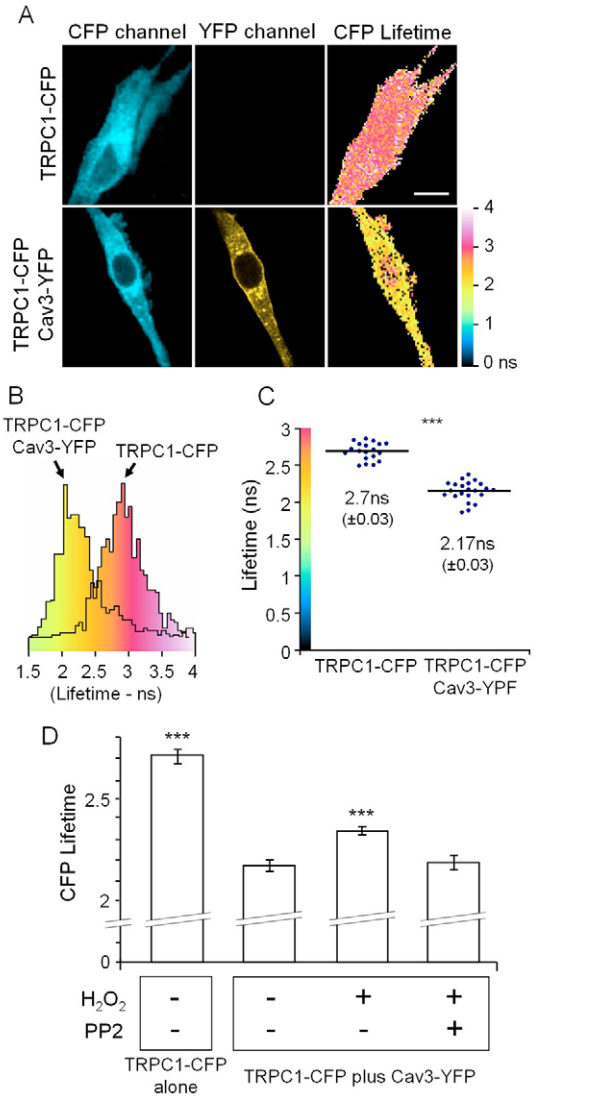

Fig. 5. CFP lifetime of TRPC1-CFP decreases when co-transfected with caveolin-3–YFP into C2 myoblasts. (A) C2 myoblasts were transfected with TRPC1-CFP alone or in combination with caveolin-3–YFP. A reduction in the CFP lifetime was detected when both plasmids were co-transfected, compared with cells transfected only with TRPC-CFP [from 2.7±0.03 nanoseconds (ns) to 2.1±0.03 ns; FRET efficiency ~20%; see B,C]. Scale bar: 10 µm. (B) Example of a lifetime measurement showing the shift of the graph to the left (shortening of lifetime) in cells co-transfected with both TRPC-CPF and caveolin-3–YFP. (C) Mean of lifetime from cells transfected with TRPC-CFP only or in combination with caveolin-3–YFP. Dots represent individual cells from three independent experiments. (D) When cells co-transfected with TRPC1-CFP and caveolin-3–YFP were incubated with H_2O_2, an increase in the CFP lifetime was detected (from 2.17 to 2.33±0.03 ns) compared with control cells (no H_2O_2). This increase was prevented by incubation of the cells with PP2 prior to H_2O_2 treatment, which shows that Src activation can induce TRPC1 conformation changes or interfere with the binding properties involved in the interaction between TRPC1 and caveolin-3 (see Discussion). Graph represents mean ± s.e.m. of a minimum of six cells per group per experiment, from three independent experiments. ***P<0.001.

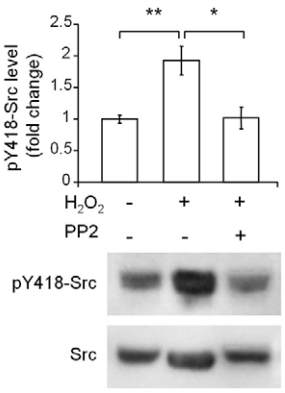

Fig. 6. H_2O_2 induces Src-kinase activation. C2 myoblasts were incubated with 10 μm H_2O_2 for 15 minutes. Immunoblots were probed for pY418-Src, striped then re-probed for total Src. A sample blot is shown. The graph represents the fold change in Src activation compared with control (pY418-Src/total Src). H_2O_2 incubation increased Src phosphorylation/activation 1.8 times compared with control cells. Such an increase was completely blocked when cells were incubated with PP2 prior to H_2O_2. Graph represents mean ± s.e.m. of four dishes per group from two independent experiments. *P<0.05; ***P<0.001.

ROS cause increased Ca^{2+} influx through SACs in *mdx* fibres

We have recently shown that the stretch-induced rise of $[Ca^{2+}]_i$ in *mdx* muscle fibres can be prevented by blockers of SACs (Yeung et al., 2005). Given that TRPC1 is a candidate protein for SACs in *mdx* muscle (Vandebrouck et al., 2002; Vandebrouck et al., 2007), we were interested to determine whether ROS could activate these channels in *mdx* muscle, as was the case for TRPC1 in our cultured C2 cells.

In the first series of experiments, we looked at the effect of the ROS scavenger 4,5-dihydroxy-1,3-benzene disulfonic acid (Tiron) on resting $[Ca^{2+}]_i$ following stretched contractions of *mdx* fibres. As shown in Fig. 8A, $[Ca^{2+}]_i$ increased almost threefold over the 20 minutes after the stretched (eccentric) contractions for control *mdx* fibres. This rise in Ca^{2+} was inhibited by 5 mM Tiron. Tetanic force after the stretched contractions was also significantly greater (~25%; P<0.05) for fibres treated with Tiron compared with controls (data not shown).

In the second series of experiments, we wanted to explore whether ROS could increase SAC activity in *mdx* muscle independently of stretch. In these experiments, we measured the change in $[Ca^{2+}]_i$ after administration of 10 μM H_2O_2 with or without the SAC blocker streptomycin (200 μM). In WT fibres, H_2O_2 had no effect on $[Ca^{2+}]_i$, whereas in *mdx* fibres there was an increase of two- to threefold (Fig. 8B). Importantly, in *mdx* fibres, $[Ca^{2+}]_i$ returned to baseline values when streptomycin was applied with H_2O_2 (see Fig. 8B), suggesting that H_2O_2 mediated the rise in $[Ca^{2+}]_i$ through the activation of SACs.

Src inhibition protects *mdx* muscle against stretch-induced damage

If SACs in *mdx* muscle are formed by TRPC1, is this channel activity regulated by Src kinase, as we had shown in the C2 cell culture experiments? To test this, we subjected isolated extensor digitorum longus (EDL) muscles from *mdx* mice to a series of stretched contractions, which we have recently shown leads to a large force deficit and ROS-dependent increase in membrane permeability in *mdx* muscle (Whitehead et al., 2008). Throughout the experiment, muscles were perfused with either the Src-kinase inhibitor PP2 or with its inactive analogue PP3. Muscle force was measured at three time points after the stretched contractions (0, 30 and 60 minutes) and compared with the pre-stretch value. At all three time points, force was significantly greater for muscles perfused with PP2 compared with PP3 (P<0.05 at 0 and 30 minutes; P<0.001 at 60 minutes). These results suggest that

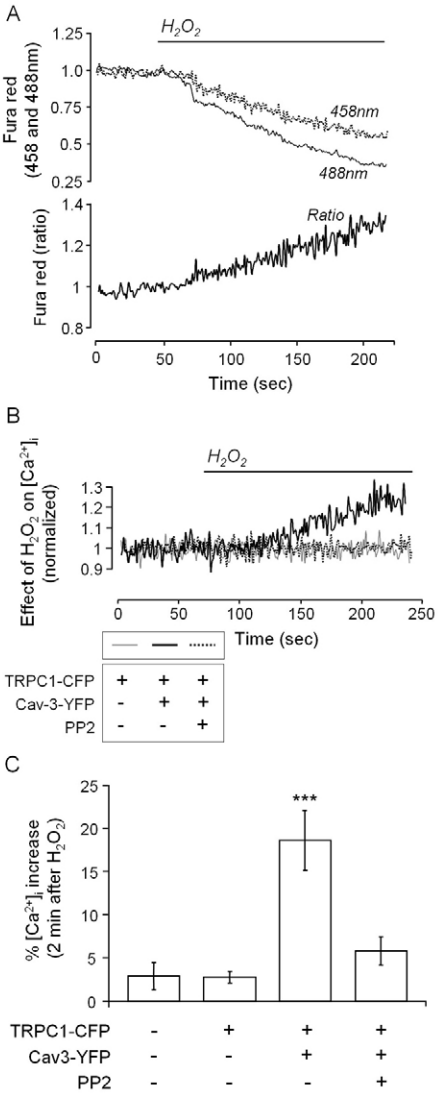

Fig. 7. TRPC1 activity depends on caveolin-3 expression and Src phosphorylation. C2 myoblasts were transfected with TRPC1-CFP alone or in combination with caveolin-3–YFP. Cells were loaded with Fura Red and imaged using scanning confocal microscopy. During imaging, cells were incubated with H_2O_2 and changes in Ca^{2+} levels were measured. (A) Fura Red is excited using the 458 nm and 488 nm laser lines (upper graph). Relative Ca^{2+} concentration is represented by the ratio of Fura Red emission upon 458 nm and 488 nm excitations (ratio=Em_{458nm}/Em_{488nm}; lower graph). (B) C2 myoblasts were co-transfected with TRPC1-CFP and caveolin-3–YFP, loaded with Fura Red, and imaged. Increase in Ca^{2+} levels, compared with control (non-transfected cells; thick black line), was detected in such cells upon H_2O_2 incubation and this increase was prevented by PP2 incubation prior to H_2O_2 treatment (dotted line). In cells expressing TRPC1-CFP only (no caveolin-3–YFP), no Ca^{2+} increase was induced by H_2O_2 incubation (thin grey line). (C) Pooled data showing the increase in Ca^{2+} influx in TRPC1–caveolin-3-expressing cells upon Src activation (by H_2O_2). Graph represents mean ± s.e.m. of a minimum of 20 cells from four independent experiments. ***P<0.001.

inhibition of Src-kinase activity provides protection against stretch-induced damage in *mdx* muscle.

Discussion

Role of Src in TRPC1 activation

Several reports describe TRPC1 activation upon Ca^{2+}-store depletion in various cell types (Wu et al., 2004; Liu et al., 2000; Zagranichnaya et al., 2005) and via different pathways (Sinkins et al., 1998; Vanden Abeele et al., 2004). Activation of TRPC1 by membrane stretch, however, has been a more controversial topic. Skeletal muscle is well-known to contain a mechanosensitive channel (Guharay and Sachs, 1984), and Maroto and colleagues proposed that TRPC1 encoded this channel (Maroto et al., 2005). In a more recent report, Gottlieb and colleagues were unable to confirm that TRPC1 expression produced a mechanosensitive channel in COS cells (Gottlieb et al., 2008). However, a weakness of these later experiments is that TRPC1 was not expressed in the plasma membrane. In our experiments, caveolin-3 expression was found to assist trafficking of TRPC1 to the plasma membrane, and TRPC1 contributed to Ca^{2+} influx only when expressed in the membrane.

In this study, we show that TRPC1 activity depends on Src phosphorylation. STIM1 and Src kinase both bind to TRPC1 (Huang et al., 2006; Kawasaki et al., 2006). Src has been shown to activate TRPC3 via phosphorylation of its N-terminus (Y226). Moreover, when TRPC3 was expressed in cells lacking Src, Fyn and Yes (Src-kinase family members), only the co-transfection of Src was able to rescue the activity of TRPC3 (Kawasaki et al., 2006). Tyrosine 226 of TRPC3, the target of Src phosphorylation, is not present in TRPC1. Nevertheless, TRPC1 has five other consensus sites for tyrosine phosphorylation in its N-terminus, including Y224 (www.cbs.dtu.dk/services/NetPhos). We have shown that the Ca^{2+} influx is six-times greater in TRPC1–caveolin-3-transfected myoblasts compared with control, and this influx was dependent on Src activation (by ROS). The FRET results might also be interpreted as evidence that Src induces the opening of TRPC1 channels (Fig. 5D). Activation of Src by H_2O_2 decreased the efficiency of FRET between TRPC1 and caveolin-3 from 20% to 14% (Fig. 5D). One possible explanation for the decrease in FRET efficiency is an increase in the distance between TPRC1 and caveolin-3, which could be either a cause or a consequence of channel opening. Caveolins generally inhibit proteins that they bind to (Williams and Lisanti, 2004); thus, reduced binding between TRPC1 and caveolin-3 might be expected to increase the activity of TRPC1. However, notwithstanding decrease in the FRET efficiency when Src became active, caveolin-3 and TRPC1 interaction was not abolished (FRET efficiency ~14%; Fig. 5D). Another possibility is that conformation changes in the TRPC1 channels (between the open and closed states) lead to the change in FRET efficiency. Kobrinsky and colleagues tagged the C- and N-termini of a K^+-gated channel with CFP and YFP, and observed a lower FRET efficiency between the subunits of the assembled channel when it became open (Kobrinsky et al., 2006). According to these authors, the decrease in FRET efficiency might reflect a conformational change in the intracellular termini that occurs during opening of the channel. Conceivably, some similar phenomenon might occur with TRPC1 upon Src activation. Thus, H_2O_2 activated Src and reduced the interaction between TRPC1 and caveolin-3, but the precise molecular rearrangement of the TRPC1–caveolin-3 complex remains uncertain.

On the basis of the observations that Src activation induced Ca^{2+} influx through TRPC1 channels (Fig. 7), we then investigated whether Src could affect TRPC1 activity via direct phosphorylation. We carried out different approaches in order to detect phosphorylation of TRPC1 by Src by using phospho-immunoprecipitation and FRET (intramolecular FRET). Neither of the techniques provided evidence of a significant increase of TRPC1 phosphorylation upon Src activation (data not shown). It remains possible that the techniques we have used are not sufficiently sensitive to detect phosphorylation of TRPC1 by endogenous Src. Indeed, Kawasaki and colleagues only detected TRPC3 phosphorylation when exogenous Src was co-transfected with TRPC3 (Kawasaki et al., 2006). Alternatively, Src might

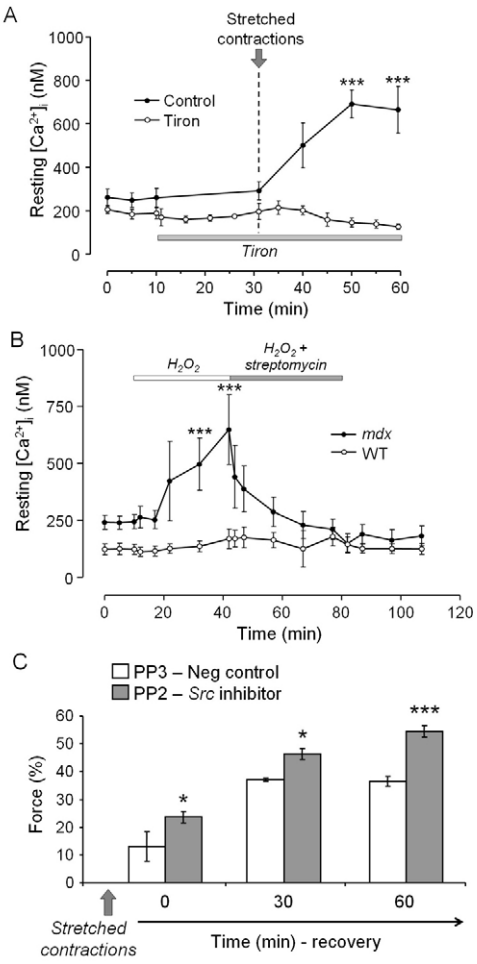

Fig. 8. Ca^{2+} influx through SACs is mediated by ROS in *mdx* fibres and Src inhibition reduces stretch-induced muscle damage in *mdx* mice. (A) Single fibres from *mdx* mice were loaded with the fluorescent Ca^{2+} indicator Fluo-4 to measure changes in $[Ca^{2+}]_i$. Fibres were then subjected to a series of ten stretched (eccentric) contractions without (control) or with the ROS scavenger Tiron (5 mM). (B) Changes in $[Ca^{2+}]_i$ in single muscle fibres from *mdx* and WT mice were measured. Following the addition of 10 μM H_2O_2 for 30 minutes, fibres were co-incubated with H_2O_2 and the SAC blocker streptomycin (200 μM) for 40 minutes, and then both drugs were washed out. (C) EDL muscle was dissected from *mdx* mice and a series of ten stretched contractions was performed. Recovery of the muscle force was measured at three time points after stretched contractions (0, 30 and 60 minutes). Compared with control muscles incubated with PP3, inhibition of Src kinase by PP2 protected *mdx* muscle from damage induced by stretched contractions. (A) n=9 for control and n=6 for Tiron; (B) n=4 for WT and n=6 for *mdx*; (C) n=3 per group. *P<0.05; **P<0.01; ***P<0.001.

regulate TRPC1 via an indirect path (activation of other kinases or cytoskeleton modifications) and our experiments do not rule out either possibility. Whether Src kinase acts directly or indirectly on TRPC1 remains to be further investigated.

We have shown here that activation of TRPC1 depends on Src-kinase phosphorylation, but a heteromeric channel containing TRPC1 might also be activated by phosphorylation of other subunits. It has been shown that TRPC1 binds to TRPC3 and that this heteromer forms a SOC (Liu et al., 2005). However, immunolabelling of TRPC3 in isolated adult muscle fibres showed an intracellular pattern that did not colocalise with TRPC1, which was present in the sarcolemma (Vandebrouck et al., 2002). TRPC4, which is also found in skeletal muscle, can bind to TRPC1 (Hofmann et al., 2002), is located in the sarcolemma (Vandebrouck et al., 2002) and is phosphorylated by Src (Odell et al., 2005). Therefore, we suspect that TRPC4 activation by Src might also participate in the activation of a TRPC1-TRPC4 heterologous channel in adult muscle fibres.

Role of caveolin-3 in TRPC1 activity

Interaction with caveolin-3 is important for the plasma membrane expression and function of TRPC1. Caveolin-1 binds to TRPC1, helping to target TRPC1 to lipid rafts and regulate its activity (Brazer et al., 2003). Caveolin-1-knockout mice showed impaired endothelial Ca^{2+} entry and a decreased interaction between TRPC1 and TRPC4, both of which were rescued by the reintroduction of caveolin-1 (Murata et al., 2007). Caveolin-1 can bind to both the N- and C-terminal ends of TRPC1, but the N-terminal interaction is responsible for targeting the channel to the plasma membrane (Brazer et al., 2003). Deletion of the N-terminus of TRPC1 prevented the surface expression of the channel and reduced store-operated Ca^{2+} entry in transfected cells. Kwiatek and colleagues reported that the caveolin-1 scaffolding domain bound to the TRPC1 C-terminus and markedly reduced Ca^{2+} influx (Kwiatek et al., 2006). Caveolin-3 is 85% similar to caveolin-1 (Tang et al., 1996) and we have shown evidence that, similar to caveolin-1 (Brazer et al., 2003), caveolin-3 also binds to TRPC1.

In addition to binding to TRPC1, caveolin-3 also assisted in the targeting of this protein to the plasma membrane when both proteins were co-expressed in myoblasts. Myoblasts transfected with only TRPC1 showed no clear plasma membrane expression, nor Ca^{2+} influx induced by Src activation. Thus, caveolins appear to play an important role in determining the plasma membrane residency (and perhaps assembly) of TRPC1 (Figs 4 and 7) (Brazer et al., 2003). Caveolin-3 might also be responsible for stabilisation of TRPC1 on the cell surface. Hernández-Deviez and colleagues (Hernández-Deviez et al., 2008) recently found that, in cells lacking caveolin-1, dysferlin on the plasma membrane was less stable. By analogy, caveolin-3 might well be important for the stabilisation of TRPC1. Once both TRPC1 and caveolin-3 are assembled in the membrane, caveolin-3 might exert a partial inhibitory effect on the activity of the TRPC1 channel, as has been observed in other systems (Kwiatek et al., 2006; Williams and Lisanti, 2004).

Role of caveolin-3, Src kinase and TRPC1 in DMD

Our data suggest that caveolin-3 expression is necessary for TRPC1 localisation. Src activation produced detectable changes in the interaction between TRCPC1 and caveolin-3 (by FRET) and stimulated opening of the TRPC1 channel. This might be important in muscular dystrophies, especially DMD, because levels of TRPC1, caveolin-3 and Src kinase were all increased in *mdx* muscle. Cell culture experiments showed that Src activation by ROS markedly increased Ca^{2+} influx in cells expressing TRPC1 and caveolin-3. Therefore, we carried out experiments on *mdx* muscle to investigate the role of ROS and Src on the activation of SACs, which might be formed by TRPC1 (Vandebrouck et al., 2002; Maroto et al., 2005; Vandebrouck et al., 2007). First, we showed that the stretch-induced Ca^{2+} influx in *mdx* fibres was prevented by the ROS scavenger Tiron, suggesting that ROS mediates SAC activity in *mdx* muscle. We then provided evidence that exogenous ROS also increased Ca^{2+} influx through SACs in *mdx*, but not WT, fibres in the absence of stretch. This result suggests that *mdx* muscle is more sensitive to ROS. This is consistent with the findings of Rando and colleagues (Rando et al., 1998), who demonstrated that *mdx* muscle is more susceptible to oxidative cell death than WT. To further investigate the possible role of Src kinase in *mdx* muscle, we carried out stretched contractions on isolated *mdx* muscles to assess the role of this protein in muscle damage. Our experiments show that Src inhibition during stretched contractions provided protection against muscle damage. Because we have previously shown that blockers of SACs prevented the rise in $[Ca^{2+}]_i$ (Williams and Allen, 2007a) and significantly improved force after stretched contractions in *mdx* muscle (Yeung et al., 2005; Whitehead et al., 2006b), our current findings lead us to hypothesise that Src inhibition might provide protection against muscle damage in *mdx* muscle owing to a reduction in Ca^{2+} influx through SACs and/or TRPC1. In addition, given that ROS can activate Src and that ROS production is increased in dystrophic muscles (Williams and Allen, 2007b; Whitehead et al., 2008), this pathway could mediate increased activity of TRPC1 in *mdx*/DMD muscle. Based on the results presented here, we suggest that targeting the ROS-Src-TRPC1/caveolin-3 pathway could lead to the development of new therapeutic approaches for the treatment of DMD.

Materials and Methods

Animals and cell culture

Male *mdx* and WT (C57BL/10ScSn) mice at 8 weeks of age were obtained from the Animal Resources Center (Perth, Australia). All experiments were approved by the Animal Ethics Committee of the University of Sydney, Australia. Murine skeletal muscle cells (C2 myoblasts) were used for the cell culture experiments and cultured as previously described (Gervásio and Phillips, 2005).

Immunoblotting and immunoprecipitation

Animals were killed with an overdose of sodium pentobarbitone (163 mg/kg of body weight) diluted in heparin (Whitehead et al., 2006a). TA muscle lysates were immunoblotted as previously described (Whitehead et al., 2008) for anti-caveolin-3 (1:2000; BD Biosciences, San Jose, CA), anti-TRPC1 (1:1000; Alomone Labs, Jerusalem, Israel), anti-Src (1:1000; Chemicon/Millipore, Billerica, MA), anti-pY418-Src (Sigma) and anti-GAPDH (1:15,000; Chemicon/Millipore). Total protein was measured using a Bradford assay (Bio-Rad, Hercules, CA). Bands were visualised with HRP-conjugated anti-mouse IgG (for caveolin, anti-Src and GAPDH) or anti-rabbit IgG (for TRPC1 and anti-pY418-Src; 1:1000; Santa Cruz, CA) (Whitehead et al., 2008). Quantification of western blots was obtained by multiplying the area and intensity of each band using ImageJ software (Whitehead et al., 2008). The graphs shown in Fig. 1 were normalised to GAPDH as a loading control (probed on the same gel).

For the IP, muscles were lysed in IP buffer containing 50 mM Tris pH7.5, 150 mM NaCl, 25 mM EDTA, 25 mM EGTA and 1% NP-40, and protease and phosphatase inhibitors (Sigma, St Louis, MO). Lysate (200 μg of protein) was first incubated with 50 μl of protein-A-Sepharose beads (Amersham Biosciences-GE Healthcare, Piscataway, NJ) for 1 hour. The beads were precipitated (800 ***g***, 3 minutes) and the supernatant (cleared lysate) was incubated with 2.5 μg of anti-TRPC1 antibody for 2.5 hours. Fresh beads (25 μl) were added to the lysate and incubated for 1 hour. The immunocomplex beads were precipitated and were washed four times with the same buffer described above containing 0.1% NP-40. The immunoprecipitate was resolved by 8% SDS-PAGE. The membranes were probed for caveolin-3 and bands were detected as described above. In a reverse IP, the lysate was incubated with anti-TRPC1 and the membrane was probed with anti-caveolin-3. All the steps of the IP were carried out at 4°C.

Immunofluorescence and image analysis

TA muscles were processed and cryosections stained for immunofluorescence as previously described (Gervásio el al., 2007) but using anti-caveolin-3 and anti-TRPC1 antibodies (overnight, 4°C) visualised with Alexa-Fluor-488-conjugated goat anti-mouse antibody (1:1000; Molecular Probes, Eugene, OR) and Cy3-conjugated goat anti-rabbit (1:250; Jackson ImmunoResearch Laboratories, West Grove, PA), respectively. Control sections were incubated with secondary antibody (no primary antibody) to confirm the absence of significant non-specific binding or fluorescence cross-bleed (data not shown). Sections were imaged with a Zeiss EC Plan-Neofluar 40× 0.75 NA dry objective by laser scanning confocal microscopy (Zeiss LSM 510 Meta). ImageJ software was used for fluorescence and colocalisation quantitation of caveolin-3 and TRPC1 (Gervásio and Phillips, 2005).

Fluorescence resonance energy transfer (FRET)

FRET between caveolin-3 and TRPC1 was tested using two independent approaches: photobleaching of acceptor (Bastiaens et al., 1996; Kenworthy, 2001) and FLIM (Cox et al., 2007). Plasmids were kindly donated by Robert Parton [caveolin-3–YFP (Pol et al., 2004)], and Thomas Hofmann and Thomas Gudermann [TRPC1-CFP (Hofmann et al., 2002)]. The identity of the plasmids was confirmed by sequencing. Immunocytochemistry of transfected cells also confirmed that the exogenously expressed proteins were indeed TRPC1 and caveolin-3 (supplementary material Fig. S2). C2 myoblasts were cultured on glass coverslips and transfected with either plasmid or a combination of both using Effectene transfecting reagent (Qiagen; Chatsworth, CA) according to manufacturer's instructions. At 48 hours after transfection, cells were washed in PBS and fixed with 2% paraformaldehyde in PBS (20 minutes, room temperature). Coverslips were mounted in DABCO anti-fade reagent (FUKA) and cells were visualised using either the Zeiss LSM 510 Meta confocal microscope (photobleaching of acceptor) or Nikon D-Eclipse C1 confocal microscope (Japan) attached to a Nikon TE2000 microscope (equipped with a High Speed Lifetime Imaging Module – LIMO/FLIM).

For photobleaching of acceptor, a region of interest (ROI) within transfected cells was selectively exposed to ten scans using the 514 nm laser line at 100% power. The whole cell was imaged at lower laser intensity (15%) for both donor and acceptor optical channels immediately before and after the bleaching of acceptor. FRET efficiency (*E*) was calculated from the increase of the fluorescence intensity of the donor after the acceptor was selectively photobleached (Bastiaens et al., 1996; Gervásio et al., 2007).

FLIM was also used to detect FRET between the tagged caveolin-3 and TRPC1. Experimentally, this can be calculated by measuring the fluorescence lifetime of the donor in the presence and absence of the acceptor using the following expression: $E=1-(tDA/tD)$, where *tDA* and *tD* are the donor lifetimes in the presence and absence of acceptor, respectively (*E*=FRET efficiency) (Bastiaens and Squire, 1999). CFP was excited by a picosecond-pulsed 405 nm laser (PicoQuant GmbH, Berlin, Germany) and emission was collected using a band-pass barrier filter (470-490 nm, Nikon). The average lifetime of each pixel was calculated by the LIMO software from images of 100×100 pixels.

Hydrogen peroxide incubations

H_2O_2 was used at 10 μM final concentration for 15 minutes in culture media for all experiments. Cells were washed once with cold PBS and lysed for immunoblot analysis of total Src and pY418-Src as described above. In a subset of dishes, the Src-kinase inhibitor PP2 (Calbiochem, San Diego, CA) was added 1 hour prior to H_2O_2 incubation.

Ratiometric Ca^{2+} imaging

Cells were grown on 35 mm glass bottom dishes (Matek, Homer, MA) and transfected with either caveolin-3–YFP, TRPC1-CFP or a combination of both plasmids as described above. Fura Red AM (Molecular Probes) was used at a final concentration of 10 μM. At 48 hours after transfection, cells were loaded with Fura Red for 45 minutes at 37°C and imaged using a Zeiss C-Apochromat 40× 1.2 NA water-immersion objective (Zeiss LSM 510 Meta). A sequential acquisition mode was set up using the 458 and 488 nm argon laser lines (four images/second; emission 636-750 nm using Meta detector). ROI were drawn around transfected and non-transfected cells, and fluorescence intensities were plotted against time using the Zeiss 510 Meta Software version 4.2. $[Ca^{2+}]_i$ is shown as a ratio of fluorescence intensities of each ROI [458 nm/488 nm (Ippolito et al., 2006)].

Ex vivo experiments on *mdx* single fibres

mdx and WT mice (8-12 weeks of age) were killed by cervical dislocation and single fibres were dissected, as described previously (Yeung et al., 2005). Single fibres were then transferred to a perspex chamber and perfused with a standard solution containing (mM): NaCl (121), KCl (5), $CaCl_2$ (1.8), $MgCl_2$ (0.5), NaH_2PO_4 (0.4), $NaHCO_3$ (24) and glucose (5.5). The solution was continuously bubbled with 95% O_2 – 5% CO_2 (pH 7.4). Experiments were performed at room temperature. Aluminium clips clamped to the tendons enabled the fibre to be attached to a force transducer and the lever of a motorised length controller. Fibres were loaded with 10 μm Fluo-4-AM (Molecular Probes), to measure the resting $[Ca^{2+}]_i$.

In the first experiments, we investigated the effect of the ROS scavenger Tiron on stretch-induced $[Ca^{2+}]_i$. *mdx* fibres underwent a series of ten stretched (eccentric) contractions, using the same stimulation and stretch protocol as described previously (Yeung et al., 2005). In some experiments, fibres were perfused with 5 mM Tiron from 20 minutes before the stretched contractions until the conclusion of the experiment (30 minutes after the stretched contractions).

In the second series of experiments, we investigated whether application of an exogenous ROS could increase $[Ca^{2+}]_i$ via SACs, independent of muscle stretch. Here, WT and *mdx* fibres were incubated with 10 μM H_2O_2 for a total of 70 minutes while $[Ca^{2+}]_i$ was measured. Fibres were initially exposed to H_2O_2 for 30 minutes and then 200 μM streptomycin, a SAC blocker, was also added to the perfusate (see Fig. 8B).

Ex vivo experiments on *mdx* muscle

EDL muscles were dissected from *mdx* mice and transferred to a perspex chamber as described above for the single-fibre experiments (for details, see Whitehead et al., 2008). The muscles were subjected to a series of ten stretched contractions, using the same protocol as described in Whitehead et al. (Whitehead et al., 2008). Before, during and after the stretched contractions, muscles were perfused with either 10 μM PP2 (a Src-kinase inhibitor) or 10 μM PP3 (an inactive analogue of PP2), which was used as a control. Maximum tetanic force (120 Hz stimulation) was measured at 0, 30 and 60 minutes after the stretched contractions and compared with pre-stretch values.

Statistics

Student's *t*-test (two-tailed) was used to compare means of two different groups. Analysis of variance (ANOVA) was used in situations of more than two groups (one-way ANOVA: Fig. 5D, Fig. 6 and Fig. 7C) or two variables (two-way ANOVA: Fig. 8). Mean and standard error of the mean (s.e.m.) are shown for each group.

We acknowledge the facilities as well as scientific and technical assistance from Ellie Kable and Renee Whan (the AMMRF Australian Microscopy & Microanalysis Facility at the Electron Microscope Unit, the University of Sydney), and Louise Cole (Bosch Institute, University of Sydney) for help with the confocal imaging. We are grateful to Robert Parton, Thomas Hofmann and Thomas Gudermann for kindly donating the plasmids used in this study. We also acknowledge funding from the National Health and Medical Research Council of Australia and Research Grants Council Grant of the Hong Kong Special Administrative Region, China (PolyU 5468/05M).

References

Abram, C. L. and Courtneidge, S. A. (2000). Src family tyrosine kinases and growth factor signaling. *Exp. Cell Res.* **254**, 1-13.

Ahmmed, G. U., Mehta, D., Vogel, S., Holinstat, M., Paria, B. C., Tiruppathi, C. and Malik, A. B. (2004). Protein kinase C-alpha phosphorylates the TRPC1 channel and regulates store-operated Ca^{2+} entry in endothelial cells. *J. Biol. Chem.* **279**, 20941-20949.

Bastiaens, P. I. and Squire, A. (1999). Fluorescence lifetime imaging microscopy: spatial resolution of biochemical processes in the cell. *Trends Cell Biol.* **9**, 48-52.

Bastiaens, P. I., Majoul, I. V., Verveer, P. J., Söling, H. D. and Jovin, T. M. (1996). Imaging the intracellular trafficking and state of the AB5 quaternary structure of cholera toxin. *EMBO J.* **15**, 4246-4253.

Brazer, S. C., Singh, B. B., Liu, X., Swaim, W. and Ambudkar, I. S. (2003). Caveolin-1 contributes to assembly of store-operated Ca^{2+} influx channels by regulating plasma membrane localization of TRPC1. *J. Biol. Chem.* **278**, 27208-27215.

Brereton, H. M., Harland, M. L., Auld, A. M. and Barritt, G. J. (2000). Evidence that the TRP-1 protein is unlikely to account for store-operated Ca^{2+} inflow in Xenopus laevis oocytes. *Mol. Cell. Biochem.* **214**, 63-74.

Chen, D. B., Li, S. M., Qian, X. X., Moon, C. and Zheng, J. (2005). Tyrosine phosphorylation of caveolin 1 by oxidative stress is reversible and dependent on the c-src tyrosine kinase but not mitogen-activated protein kinase pathways in placental artery endothelial cells. *Biol. Reprod.* **73**, 761-772.

Chen, K., Vita, J. A., Berk, B. C. and Keaney, J. F., Jr (2001). c-Jun N-terminal kinase activation by hydrogen peroxide in endothelial cells involves SRC-dependent epidermal growth factor receptor transactivation. *J. Biol. Chem.* **276**, 16045-16050.

Cox, G., Matz, M. and Salih A. (2007). Fluorescence lifetime imaging of coral fluorescent proteins. *Microsc. Res. Tech.* **70**, 243-251.

Dietrich, A., Kalwa, H., Storch, U., Mederos, Y., Schnitzler, M., Salanova, B., Pinkenburg, O., Dubrovska, G., Essin, K., Gollasch, M. et al. (2007). Pressure-induced and store-operated cation influx in vascular smooth muscle cells is independent of TRPC1. *Pflugers Arch.* **455**, 465-477.

Ducret, T., Vandebrouck, C., Cao, M. L., Lebacq, J. and Gailly, P. (2006). Functional role of store-operated and stretch-activated channels in murine adult skeletal muscle fibres. *J. Physiol.* **575**, 913-924.

Engelman, J. A., Zhang, X., Galbiati, F., Volonte, D., Sotgia, F., Pestell, R. G., Minetti, C., Scherer, P. E., Okamoto, T. and Lisanti, M. P. (1998). Molecular genetics of the caveolin gene family: implications for human cancers, diabetes, Alzheimer disease, and muscular dystrophy. *Am. J. Hum. Genet.* **63**, 1578-1587.

Galbiati, F., Volonte, D., Engelman, J. A., Scherer, P. E. and Lisanti, M. P. (1999). Targeted down-regulation of caveolin-3 is sufficient to inhibit myotube formation in differentiating C2C12 myoblasts. *J. Biol. Chem.* **274**, 30315-30321.

Galbiati, F., Volonte, D., Chu, J. B., Li, M., Fine, S. W., Fu, M., Bermudez, J., Pedemonte, M., Weidenheim, K. M., Pestell, R. G. et al. (2000). Transgenic overexpression of caveolin-3 in skeletal muscle fibers induces a Duchenne-like muscular dystrophy phenotype. *Proc. Natl. Acad. Sci. USA* **97**, 9689-9694.

Gervásio, O. L. and Phillips, W. D. (2005). Increased ratio of rapsyn to ACh receptor stabilizes postsynaptic receptors at the mouse neuromuscular synapse. *J. Physiol*. **562**, 673-685.

Gervásio, O. L., Armson, P. F. and Phillips, W. D. (2007). Developmental increase in the amount of rapsyn per acetylcholine receptor promotes postsynaptic receptor packing and stability. *Dev. Biol.* **305**, 262-275.

Gottlieb, P., Folgering, J., Maroto, R., Raso, A., Wood, T. G., Kurosky, A., Bowman, C., Bichet, D., Patel, A., Sachs, F. et al. (2008). Revisiting TRPC1 and TRPC6 mechanosensitivity. *Pflugers Arch*. **455**, 1097-1103.

Guharay, F. and Sachs, F. (1984). Stretch-activated single ion channel currents in tissue-cultured embryonic chick skeletal muscle. *J. Physiol*. **352**, 685-701.

Hernández-Deviez, D. J., Howes, M. T., Laval, S. H., Bushby, K., Hancock, J. F. and Parton, R. G. (2008). Caveolin regulates endocytosis of the muscle repair protein, dysferlin. *J. Biol. Chem*. **283**, 6476-6488.

Hisatsune, C., Kuroda, Y., Nakamura, K., Inoue, T., Nakamura, T., Michikawa, T., Mizutani, A. and Mikoshiba, K. (2004). Regulation of TRPC6 channel activity by tyrosine phosphorylation. *J. Biol. Chem*. **279**, 18887-18894.

Hoffman, E. P., Brown, R. H., Jr and Kunkel, L. M. (1987). Dystrophin: the protein product of the Duchenne muscular dystrophy locus. *Cell* **51**, 919-928.

Hofmann, T., Schaefer, M., Schultz, G. and Gudermann, T. (2002). Subunit composition of mammalian transient receptor potential channels in living cells. *Proc. Natl. Acad. Sci. USA* **99**, 7461-7466.

Huang, G. N., Zeng, W., Kim, J. Y., Yuan, J. P., Han, L., Muallem, S. and Worley, P. F. (2006). STIM1 carboxyl-terminus activates native SOC, I(crac) and TRPC1 channels. *Nat. Cell Biol*. **8**, 1003-1010.

Ippolito, J. E., Merritt, M. E., Bäckhed, F., Moulder, K. L., Mennerick, S., Manchester, J. K., Gammon, S. T., Piwnica-Worms, D. and Gordon, J. I. (2006). Linkage between cellular communications, energy utilization, and proliferation in metastatic neuroendocrine cancers. *Proc. Natl. Acad. Sci. USA* **103**, 12505-12510.

Ju, Y. K., Chu, Y., Chaulet, H., Lai, D., Gervásio, O. L., Graham, R. M., Cannell, M. B. and Allen, D. G. (2007). Store-operated Ca^{2+} influx and expression of TRPC genes in mouse sinoatrial node. *Circ. Res*. **100**, 1605-1614.

Jung, C., Martins, A. S., Niggli, E. and Shirokova, N. (2008). Dystrophic cardiomyopathy: amplification of cellular damage by Ca^{2+} signaling and reactive oxygen species-generating pathways. *Cardiovasc. Res*. **77**, 766-773.

Kawasaki, B. T., Liao, Y. and Birnbaumer, L. (2006). Role of Src in C3 transient receptor potential channel function and evidence for a heterogeneous makeup of receptor- and store-operated Ca^{2+} entry channels. *Proc. Natl. Acad. Sci. USA* **103**, 335-340.

Kelly, S. M., Vanslyke, J. K. and Musil, L. S. (2007). Regulation of ubiquitin-proteasome system mediated degradation by cytosolic stress. *Mol. Biol. Cell* **18**, 4279-4291.

Kenworthy, A. K. (2001). Imaging protein-protein interactions using fluorescence resonance energy transfer microscopy. *Methods* **24**, 289-296.

Kobrinsky, E., Stevens, L., Kazmi, Y., Wray, D. and Soldatov, N. M. (2006). Molecular rearrangements of the Kv2.1 potassium channel termini associated with voltage gating. *J. Biol. Chem*. **281**, 19233-19240.

Kumar, B., Dreja, K., Shah, S. S., Cheong, A., Xu, S. Z., Sukumar, P., Naylor, J., Forte, A., Cipollaro, M., McHugh, D. et al. (2006). Upregulated TRPC1 channel in vascular injury in vivo and its role in human neointimal hyperplasia. *Circ. Res*. **98**, 557-563.

Kwiatek, A. M., Minshall, R. D., Cool, D. R., Skidgel, R. A., Malik, A. B. and Tiruppathi, C. (2006). Caveolin-1 regulates store-operated Ca^{2+} influx by binding of its scaffolding domain to transient receptor potential channel-1 in endothelial cells. *Mol. Pharmacol*. **70**, 1174-1183.

Li, S., Couet, J. and Lisanti, M. P. (1996). Src tyrosine kinases, Galpha subunits, and H-Ras share a common membrane-anchored scaffolding protein, caveolin. Caveolin binding negatively regulates the auto-activation of Src tyrosine kinases. *J. Biol. Chem*. **271**, 29182-29190.

Liu, X., Wang, W., Singh, B. B., Lockwich, T., Jadlowiec, J., O'Connell, B., Wellner, R., Zhu, M. X. and Ambudkar, I. S. (2000). Trp1, a candidate protein for the store-operated $Ca^{(2+)}$ influx mechanism in salivary gland cells. *J. Biol. Chem*. **275**, 3403-3411.

Liu, X, Bandyopadhyay, B. C., Singh, B. B., Groschner, K. and Ambudkar, I. S. (2005). Molecular analysis of a store-operated and 2-acetyl-sn-glycerol-sensitive non-selective cation channel. Heteromeric assembly of TRPC1-TRPC3. *J. Biol. Chem.* **280**, 21600-21606.

Lockwich, T. P., Liu, X., Singh, B. B., Jadlowiec, J., Weiland, S. and Ambudkar, I. S. (2000). Assembly of Trp1 in a signaling complex associated with caveolin-scaffolding lipid raft domains. *J. Biol. Chem*. **275**, 11934-11942.

Mariol, M. C. and Ségalat, L. (2001). Muscular degeneration in the absence of dystrophin is a calcium-dependent process. *Curr. Biol*. **11**, 1691-1694.

Maroto, R., Raso, A., Wood, T. G., Kurosky, A., Martinac, B. and Hamill, O. P. (2005). TRPC1 forms the stretch-activated cation channel in vertebrate cells. *Nat. Cell Biol*. **2**, 179-185.

Minetti, C., Sotgia, F., Bruno, C., Scartezzini, P., Broda, P., Bado, M., Masetti, E., Mazzocco, M., Egeo, A., Donati, M. A. et al. (1998). Mutations in the caveolin-3 gene cause autosomal dominant limb-girdle muscular dystrophy. *Nat. Genet*. **18**, 365-368.

Murata, T., Lin, M. I., Stan, R. V., Bauer, P. M., Yu, J. and Sessa, W. C. (2007). Genetic evidence supporting caveolae microdomain regulation of calcium entry in endothelial cells. *J. Biol. Chem*. **282**, 16631-16643.

Odell, A. F., Scott, J. L. and Van Helden, D. F. (2005). Epidermal growth factor induces tyrosine phosphorylation, membrane insertion, and activation of transient receptor potential channel 4. *J. Biol. Chem.* **280**, 37974-37987.

Pani, B., Cornatzer, E., Cornatzer, W., Shin, D. M., Pittelkow, M. R., Hovnanian, A., Ambudkar, I. S. and Singh, B. B. (2006). Up-regulation of transient receptor potential canonical 1 (TRPC1) following sarco(endo)plasmic reticulum Ca^{2+} ATPase 2 gene silencing promotes cell survival: a potential role for TRPC1 in Darier's disease. *Mol. Biol. Cell* **17**, 4446-4458.

Patterson, G. H., Piston, D. W. and Barisas, B. G. (2000). Förster distances between green fluorescent protein pairs. *Anal. Biochem*. **284**, 438-440.

Pol, A., Martin, S., Fernandez, M. A., Ferguson, C., Carozzi, A., Luetterforst, R., Enrich, C. and Parton, R. G. (2004). Dynamic and regulated association of caveolin with lipid bodies: modulation of lipid body motility and function by a dominant negative mutant. *Mol. Biol. Cell* **15**, 99-110.

Poteser, M., Graziani, A., Rosker, C., Eder, P., Derler, I., Kahr, H., Zhu, M. X., Romanin, C. and Groschner, K. (2006). TRPC3 and TRPC4 associate to form a redox-sensitive cation channel. Evidence for expression of native TRPC3-TRPC4 heteromeric channels in endothelial cells. *J. Biol. Chem*. **281**, 13588-13595.

Rando, T. A., Disatnik, M. H., Yu, Y. and Franco, A. (1998). Muscle cells from *mdx* mice have an increased susceptibility to oxidative stress. *Neuromuscul. Disord*. **8**, 14-21.

Rao, J. N., Platoshyn, O., Golovina, V. A., Liu, L., Zou, T., Marasa, B. S., Turner, D. J., Yuan, J. X. and Wang, J. Y. (2006). TRPC1 functions as a store-operated Ca^{2+} channel in intestinal epithelial cells and regulates early mucosal restitution after wounding. *Am. J. Physiol. Gastrointest. Liver Physiol*. **290**, G782-G792.

Sato, K., Ogawa, K., Tokmakov, A. A., Iwasaki, T. and Fukami, Y. (2001). Hydrogen peroxide induces Src family tyrosine kinase-dependent activation of Xenopus eggs. *Dev. Growth Differ*. **43**, 55-72.

Sinkins, W. G., Estacion, M. and Schilling, W. P. (1998). Functional expression of TrpC1: a human homologue of the Drosophila Trp channel. *Biochem. J*. **331**, 331-339.

Song, K. S., Scherer, P. E., Tang, Z., Okamoto, T., Li, S., Chafel, M., Chu, C., Kohtz, D. S. and Lisanti, M. P. (1996). Expression of caveolin-3 in skeletal, cardiac, and smooth muscle cells. Caveolin-3 is a component of the sarcolemma and co-fractionates with dystrophin and dystrophin-associated glycoproteins. *J. Biol. Chem.* **271**, 15160-15165.

Sours, S., Du, J., Chu, S., Ding, M., Zhou, X. J. and Ma, R. (2006). Expression of canonical transient receptor potential (TRPC) proteins in human glomerular mesangial cells. *Am. J. Physiol. Renal Physiol*. **290**, F1507-F1515.

Spencer, M. J., Croall, D. E. and Tidball, J. G. (1995). Calpains are activated in necrotic fibers from *mdx* dystrophic mice. *J. Biol. Chem*. **270**, 10909-10914.

Suzaki, Y., Yoshizumi, M., Kagami, S., Koyama, A. H., Taketani, Y., Houchi, H., Tsuchiya, K., Takeda, E. and Tamaki, T. (2002). Hydrogen peroxide stimulates c-Src-mediated big mitogen-activated protein kinase 1 (BMK1) and the MEF2C signaling pathway in PC12 cells, potential role in cell survival following oxidative insults. *J. Biol. Chem*. **277**, 9614-9621.

Sweeney, M., McDaniel, S. S., Platoshyn, O., Zhang, S., Yu, Y., Lapp, B. R., Zhao, Y., Thistlethwaite, P. A. and Yuan, J. X. (2002). Role of capacitative Ca^{2+} entry in bronchial contraction and remodeling. *J. Appl. Physiol*. **92**, 1594-1602.

Tang, Z., Scherer, P. E., Okamoto, T., Song, K., Chu, C., Kohtz, D. S., Nishimoto, I., Lodish, H. F. and Lisanti, M. P. (1996). Molecular cloning of caveolin-3, a novel member of the caveolin gene family expressed predominantly in muscle. *J. Biol. Chem*. **271**, 2255-2261.

Thomas, S. M. and Brugge, J. S. (1997). Cellular functions regulated by Src family kinases. *Annu. Rev. Cell. Dev. Biol*. **13**, 513-609.

Vaghy, P. L., Fang, J., Wu, W. and Vaghy, L. P. (1998). Increased caveolin-3 levels in *mdx* mouse muscles. *FEBS Lett*. **431**, 125-127.

Vandebrouck, A., Sabourin, J., Rivet, J., Balghi, H., Sebille, S., Kitzis, A., Raymond, G., Cognard, C., Bourmeyster, N. and Constantin, B. (2007). Regulation of capacitative calcium entries by alpha1-syntrophin: association of TRPC1 with dystrophin complex and the PDZ domain of alpha1-syntrophin. *FASEB J*. **21**, 608-617.

Vandebrouck, C., Martin, D., Colson-Van Schoor, M., Debaix, H. and Gailly, P. (2002). Involvement of TRPC in the abnormal calcium influx observed in dystrophic (*mdx*) mouse skeletal muscle fibers. *J. Cell Biol*. **158**, 1089-1096.

Vanden Abeele, F., Lemonnier, L., Thébault, S., Lepage, G., Parys, J. B., Shuba, Y., Skryma, R. and Prevarskaya, N. (2004). Two types of store-operated Ca^{2+} channels with different activation modes and molecular origin in LNCaP human prostate cancer epithelial cells. *J. Biol. Chem*. **279**, 30326-30337.

Vazquez, G., Wedel, B. J., Kawasaki, B. T., Bird, G. S. and Putney, J. W., Jr (2004). Obligatory role of Src kinase in the signaling mechanism for TRPC3 cation channels. *J. Biol. Chem*. **279**, 40521-40528.

Venkatachalam, K. and Montell, C. (2007). TRP channels. *Annu. Rev. Biochem*. **76**, 387-417.

Whitehead, N. P., Yeung, E. W. and Allen, D. G. (2006a). Muscle damage in *mdx* (dystrophic) mice: role of calcium and reactive oxygen species. *Clin. Exp. Pharmacol. Physiol*. **33**, 657-662.

Whitehead, N. P., Streamer, M., Lusambili, L. I., Sachs, F. and Allen, D. G. (2006b). Streptomycin reduces stretch-induced membrane permeability in muscles from *mdx* mice. *Neuromuscul. Disord*. **16**, 845-854.

Whitehead, N. P., Pham, C., Gervásio, O. L. and Allen, D. G. (2008). N-acetylcysteine ameliorates skeletal muscle pathophysiology in *mdx* mice. *J. Physiol*. **586**, 2003-2014.

Williams, I. A. and Allen, D. G. (2007a). Intracellular calcium handling in ventricular myocytes from *mdx* mice. *Am. J. Physiol. Heart Circ. Physiol*. **292**, H846-H855.

Williams, I. A. and Allen, D. G. (2007b). The role of reactive oxygen species in the hearts of dystrophin-deficient *mdx* mice. *Am. J. Physiol. Heart Circ. Physiol*. **293**, H1969-H1977.

Williams, T. M. and Lisanti, M. P. (2004). The Caveolin genes: from cell biology to medicine. *Ann. Med*. **36**, 584-595.

Wu, X., Zagranichnaya, T. K., Gurda, G. T., Eves, E. M. and Villereal, M. L. (2004). A TRPC1/TRPC3-mediated increase in store-operated calcium entry is required for differentiation of H19-7 hippocampal neuronal cells. *J. Biol. Chem.* **279**, 43392-43402.

Yeung, E. W., Whitehead, N. P., Suchyna, T. M., Gottlieb, P. A., Sachs, F. and Allen, D. G. (2005). Effects of stretch-activated channel blockers on $[Ca^{2+}]_i$ and muscle damage in the *mdx* mouse. *J. Physiol.* **562**, 367-380.

Zagranichnaya, T. K., Wu, X. and Villereal, M. L. (2005). Endogenous TRPC1, TRPC3, and TRPC7 proteins combine to form native store-operated channels in HEK-293 cells. *J. Biol. Chem.* **280**, 29559-29569.

Zheng, X. and Bollinger Bollag, W. (2003). Aquaporin 3 colocates with phospholipase d2 in caveolin-rich membrane microdomains and is downregulated upon keratinocyte differentiation. *J. Invest. Dermatol.* **121**, 1487-1495.